Hot electron generation via vacuum heating process in femtosecond laser–solid interactions

L. M. Chen, J. Zhang, Q. L. Dong, H. Teng, T. J. Liang, L. Z. Zhao, and Z. Y. Wei

Citation: Physics of Plasmas **8**, 2925 (2001); doi: 10.1063/1.1371956
View online: http://dx.doi.org/10.1063/1.1371956
View Table of Contents: http://scitation.aip.org/content/aip/journal/pop/8/6?ver=pdfcov
Published by the AIP Publishing

Hot electron generation via vacuum heating process in femtosecond laser–solid interactions

L. M. Chen, J. Zhang,[a] Q. L. Dong, H. Teng, T. J. Liang, L. Z. Zhao, and Z. Y. Wei
Laboratory of Optical Physics, Institute of Physics, Chinese Academy of Sciences, Beijing 100080, People's Republic of China

(Received 16 August 2000; accepted 9 March 2001)

Hot electron generation by the vacuum heating process has been studied in the interaction of 150 fs, 5 mJ, 800 nm *P*-polarized laser pulses with solid targets. The measurements have suggested that the ''vacuum heating'' is the main heating process for the hot electrons with high energies. The energy of the vacuum-heated hot electrons has been found to be higher than the prediction from the scaling law of resonance absorption. Particle-in-cell simulations have confirmed that the hot electrons are mainly generated by the vacuum heating process under certain experimental conditions. © *2001 American Institute of Physics.* [DOI: 10.1063/1.1371956]

I. INTRODUCTION

Rapid developments in intense ultrashort laser technology,[1] have opened a new regime of laser–matter interaction, in which intense laser pulses deposit their energy into solid targets faster than the hydrodynamic expansion of the target surface.[2] Thus, using table-top ultrashort pulse lasers, it is now possible to study laser–matter interaction under extreme conditions in relation to the fast ignition scheme for inertial confinement fusion (ICF),[3] harmonic generation,[4,5] ultrashort x-ray generation[6] and laser-cluster Coulumb explosions,[7] etc.

Hot electrons in laser-plasmas can be generated by different absorption or acceleration mechanisms under different experimental conditions.[8–11] Previous measurements[8] of the absorption of laser pulses by solid targets showed that at low laser intensities inverse Bremsstrahlung (IB) is the main absorption mechanism, which depends on the electrical conductivity associated with electron mean-free-path comparable to the interatomic spacing. The measurements showed three distinct regions as a function of laser intensity. At low intensities $I<10^{13}\,\mathrm{W/cm^2}$, the absorption was quite high. For an intensity in the range of $10^{13}\,\mathrm{W/cm^2}<I<10^{14}\,\mathrm{W/cm^2}$, the absorption decreased as the laser intensity increased. The absorption then increased with laser intensity for an intensity $>3\times10^{14}\,\mathrm{W/cm^2}$. These measurements are broadly consistent with collisional absorption theory. Another experiment[9] showed that at high intensities of $3\times10^{15}\,\mathrm{W/cm^2}$, the absorption was at a low level of 10% and practically independent of the target material. This behavior was attributed to the high reflection from an over-dense plasma layer caused by the rapid ionization of a thin front layer of the target. Brunel[10] proposed over ten years ago that moderately intense *P*-polarized laser pulses incident obliquely on an atomically abrupt metal surface could be strongly absorbed by pulling electrons into vacuum during an optical cycle, then returning them to the surface with approximately the quiver velocity. This is the so-called vacuum heating process. Later simulations[11] by Paul Gibbon predicted that, with a slight surface expansion of scale lengths, the laser optical field would pull more electrons into the vacuum and the laser energy would be more strongly absorbed, as long as the scale length $L=(\partial \ln n_e/\partial z)^{-1}$ does not significantly exceed the electron quiver amplitude $x_{\mathrm{osc}}=eE/m\omega^2$.

Recently, hot electron generation was studied at moderate intensities.[12,13] Both hot electron spectra and x-ray spectra from the Bremsstrahlung radiation, when hot electrons undergo de-acceleration in solid targets, showed that, when smooth solid targets were irradiated obliquely by *P*-polarized laser pulses, a group of hot electrons can be resonantly heated to a quasi-Maxwellian temperature characterized by the scaling: $T_h\propto(I\lambda^2)^{1/3}$,[14] while another group of hot electrons with higher energies can be produced by nonlinear resonant absorption if there is a thin layer of corona preplasma in front of the target surface. Typically electrons produced by the IB absorption process are known as thermal electrons and have energies less than keV at modest laser intensities.[9] The electrons generated by resonance absorption and the other nonlinear resonant absorption are called hot electrons, that have much higher kinetic energies.

In this paper, we report a study on hot electron generation from aluminum solid targets irradiated by intense ultrashort laser pulses. The measurements of the laser absorption suggested that the vacuum heating (VH) was responsible for the generation of the hot electrons with high energies. Particle-in-cell (PIC) simulations also showed that the electron spectrum generated by the vacuum heating process is consistent with the experimental results.

II. EXPERIMENTAL SETUP

The experiments were carried out at the Laboratory of Optical Physics of the Institute of Physics with a Ti:Sapphire chirped pulse amplification (CPA) laser system operating at around 800 nm at a repetition rate of 10 Hz. The laser delivered 5 mJ energy in 150 fs pulses and produced a peak irradiance of $8\times10^{15}\,\mathrm{W/cm^2}$ at the focus. The contrast ratio of

[a]Author to whom correspondence should be addressed. Electronic mail: jzhang@aphy.iphy.ac.cn

the laser pulses was measured to be $\sim 10^{-5}$ at 2 ps before the peak and 10^{-6} at 1 ns, by third-order autocorrelation techniques. The target material used was 100 μm thick pure Al on glass plates. The roughness of the surface was less than 1 μm. The target mount was controlled by step-motors in xyz dimension to ensure the laser pulses interacted with a fresh target surface for each shot.

The main diagnostic of the hot electrons was a magnetic spectrometer, fitted with a permanent magnetic field of $B = 380$ Gauss. An array of LiF thermoluminescent dosimeters (TLDs) was used as detectors. Recent development of ultrasensitive LiF TLD material provides the possibility of using a thin TLD for hot electron detection.[15] The energy range this instrument covered was from 7 to 500 keV. The collection angle of the spectrometer was on the order of 1×10^{-3} Steradiant. Its energy resolution was better than 2%. Because the TLDs are insensitive to visible light, it was not necessary to use aluminum foils in front of the TLDs. The background of these TLDs was less than 1.2 μGy when they were heated to 240 °C. When we placed a piece of 20 μm Al foil on the surface of the TLD, which was located in the position of the spectrometer, corresponding to an energy of 20 keV, the dose on the TLDs would drop dramatically from several tens of mGy to several μGy. This verified that the dose on the TLDs was mainly caused by hot electrons.

Two calibrated γ-ray spectrometers were also used to study the x-ray Bremsstrahlung radiation from the laser–plasma.[13] The γ-ray spectrometer consisted of a NaI detector, an electronic gated shutter, a photomultiplier, an amplifier and a multichannel energy analyzer. A 20 mm diameter hole in a 50 mm thick Pb block was used to collimate the x-ray radiation and to shield the detector. The detector response was calibrated using a 511 keV and a 1.274 MeV γ-ray ^{22}Na source and a 665 keV ^{137}Cs source.

The plasma absorption was measured by a calorimeter. Slightly focusing (with an f/10 lens) of the reflected beam ensured that the whole beam was collected by the calorimeter. An 800 nm filter was placed at the entrance of the calorimeter ensured only the reflected and scattered laser energy could be measured.

III. ABSORPTION MEASUREMENTS

All of the experimental results presented here were obtained for laser pulses incident on the target at an angle of 45° with respect to the normal of Al targets.

The measurement of reflectivity (solid dots) from the target is shown in Fig. 1 for different focused laser intensities on the target. The scattered light out of the collecting optics was found to be negligible. When the focused laser intensity was 5×10^{12} W/cm^2, no hard x-ray photons could be detected. The measured reflectivity was found to be as high as 80%. This is consistent with the previous measurements,[8] in which the IB absorption was believed to take a major role. As the laser intensity was increased from $I>3\times10^{13}$ W/cm^2, x-ray photons began to be detectable and the x-ray flux and photon energy increased with the laser intensity. In the meantime, the measured reflectivity decreased for higher laser intensities. This implies that there were other

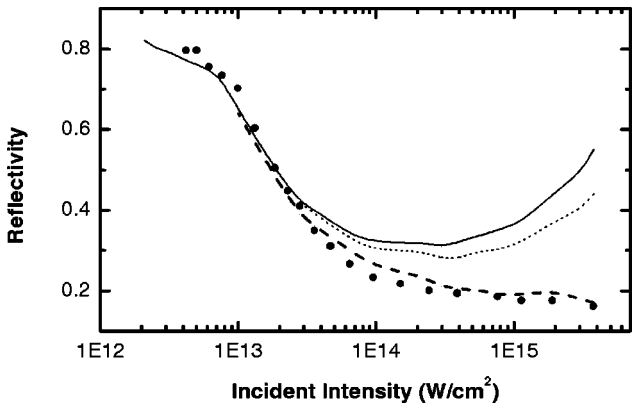

FIG. 1. The laser reflectivity (solid circle) vs laser intensity on Al target for P-polarized 45° irradiation. The solid line is from calculation of IB absorption with Fresnel–Drude formulas. The dotted line is the IB absorption plus the VH absorption with $\eta=6$ (without plasma expansion). The dashed line is the IB absorption plus the VH absorption with $\eta=20$ (with slight plasma expansion).

absorption mechanisms starting to play a role, which generated the hot electrons. Compared with the calculated results using the Fresnel–Drude formula with Perrot and Dharmawardana's conductivity model[8] (shown in Fig. 1, by the solid line), we can see that our measurements also began to deviate from the previous measurements[8] and the calculation from $I>3\times10^{13}$ W/cm^2. Increasingly more energy was absorbed through other mechanisms for higher laser intensities. At an intensity of 4×10^{15} W/cm^2, the total absorption was as high as more than 80%, in which nearly 40% extra laser energy was absorbed through other mechanisms.

Unlike the calculation from the Fresnel–Drude formula or the previous experimental results,[8] in which IB was the main absorption mechanism, it can be seen that the extra absorption, therefore the total absorption, increased with the laser intensity. This behavior is consistent with Grimes measurements[16] using femtosecond time-resolved reflectivity.

We can now investigate the possible mechanisms for the extra absorption in the measurements. The laser pulse duration was 150 fs and the pedestal was not enough to generate significant plasma expansion before the peak of the laser pulse.[17] The plasma scale-length was measured to be below 0.01 λ using a shadowgraphy technique. The electron quiver amplitude under the experimental laser intensity was $X_{\rm osc}/\lambda\sim0.02$. Therefore, the plasma scale length was satisfied with the requirements of the VH heating process.

There are other competing linear absorption mechanisms, such as anomalous skin effect (ASE),[18] sheath inverse Bremsstrahlung (SIB),[19] sheath transit absorption (STA),[20] and resonance absorption (RA)[14] in the laser–plasma interactions. If we choose an intensity of $I=10^{15}$ W/cm^2, for example, the peak electron temperature of $kT_e\sim100$ eV, this would result in a collision frequency $\nu\sim5\times10^{15}$ s^{-1}. The skin depth in our experiment is $l_s\sim10\nu_{\rm th}/\nu$.[21] This is much thicker than the required collisionless transit of the skin depth ($l_s\sim100$ Å$\ll\nu_{\rm th}/\nu$) for efficient ASE, SIB, and STA absorption processes. Therefore, the ASE, SIB, and STA processes contribute very little to the absorption under our

experimental conditions. On the other hand, the RA absorption involves a slow, many-cycle building up of a resonant plasma wave, which eventually breaks, and an electric field at the critical surface. For the steep plasma gradients in our experiments, the building up time might be too short for RA to efficiently enhance the critical surface field. Paul Gibbon's simulation[11] showed that the VH dominates over the resonance absorption for scale lengths of $L/\lambda < 0.1$. According to his simulations, the absorbed energy goes into two kinds of hot electrons. A bi-Maxwellian distribution will be formed by the electrons heated, within the laser penetration depth, by the RA absorption process, and the VH heated electrons with much higher energies, escaped from the high-density boundary.

In principle, the VH absorption can be distinguished from other competing linear mechanisms by its intrinsic intensity dependence $f_{\mathrm{VH}} \sim \sqrt{I\lambda^2}$ and its unique incident angle and polarization dependence. From Fig. 1, we can find that the extra energy absorption is mainly due to the VH process because of the intensity dependence, as described by Brunel equation. The fractional VH absorption is

$$f_{\mathrm{VH}} = (\eta/2\pi)(v_{\mathrm{osc}}^3/v_L^2 c \cos\theta), \tag{1}$$

where $v_L = eE_L/m\omega$ is the electron velocity in the incident laser field (E_L is the incident laser electric field) and v_{osc} is the quiver velocity due to the total electric field of incident and reflected fields $E_0 = \xi E_L \sin\theta$. Here $\eta = 1.75(1 + 2v_{\mathrm{th}}/v_{\mathrm{osc}})$ is an empirical scaling value determined by the density gradient.[10] In order to compare the fractional VH absorption and the measurements in Fig. 1, the fractional absorption from IB should be considered. The solid line in Fig. 1 is the calculation from the IB collisional theory. It is apparent that the absorption in our experiments was mainly the IB absorption for laser intensities of $I < 3\times10^{13}\,\mathrm{W/cm^2}$, while some other absorption mechanisms played roles for higher laser intensities $I > 3\times10^{13}\,\mathrm{W/cm^2}$. If we assume there was no hydrodynamic expansion in the interaction ($\eta = 6$), the total energy absorption (VH+IB) would be much lower than the experimental data (as the dotted line shows in Fig. 1). This implies that the ideal abrupt density gradient without any plasma expansion does not fit for our experimental situation. If we assume that there is a slight plasma expansion so that we can assume $\eta = 20$, just as Grimes did,[16] in the empirical scaling value, the total energy absorption curve (the dashed line in Fig. 1) will be very close to the experiment data. This change is more realistic for experiments because a slight plasma expansion will build at the pedestal of the laser pulse anyway. As a result, we found the extra absorption is nearly 40% at the intensity $4\times10^{15}\,\mathrm{W/cm^2}$. This calculation based on Brunel's VH intensity dependence $f_{\mathrm{VH}} \propto \sqrt{I\lambda^2}$. However, if we choose Grimes' intensity dependence $f_{\mathrm{VH}} \propto (I\lambda^2)^{0.64}$,[16] the extra absorption would be nearly 55%, beyond the difference between experimental data and IB value under the intensity of $4\times10^{15}\,\mathrm{W/cm^2}$. Therefore, we found that Brunel's VH laser intensity dependence is more reliable.

From this comparison, we can find: (1) The VH is the main absorption mechanism apart from the IB absorption in our experiments, especially at high intensities, because the VH absorption is proportional to the square root of laser intensity. (2) The measured absorption is somewhat larger than Brunel's idealized case. This supports the assumption of enhancement of VH absorption for a slightly expanded plasma[11] because the laser field can penetrate further into the surface and can pull more electrons into the VH orbits. As a result, electrons will have a longer mean-free-path in the plasma to gain higher energies. Paul Gibbon predicted a 60% VH absorption[22] for an expanded plasma at an intensity of $4\times10^{15}\,\mathrm{W/cm^2}$. This is more or less similar to our experiment data.

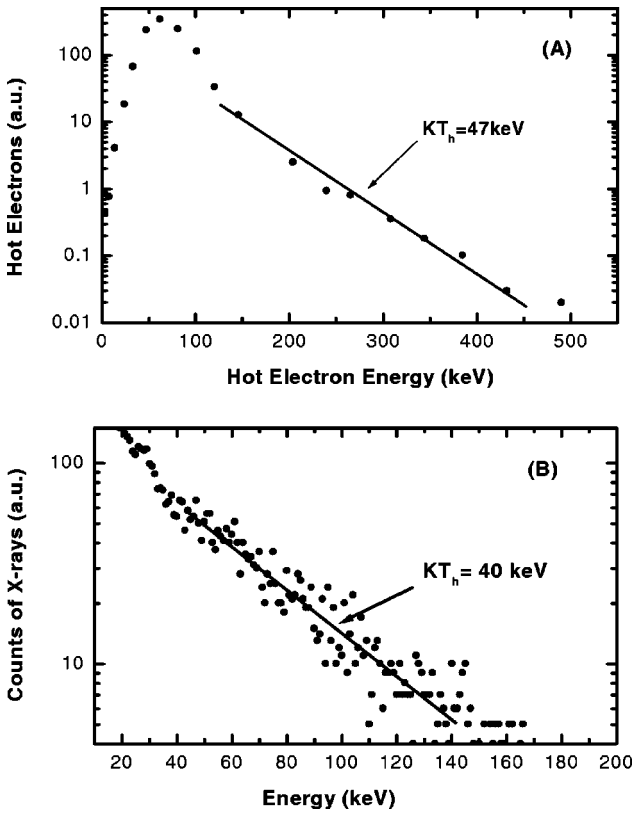

FIG. 2. (A) The energy spectrum of hot electrons emission and (B) the Bremsstrahlung hard x-ray radiation from the Al target. The solid lines in two figures are the Maxwellian distribution fit for the temperature.

The optimum incident angle for maximum absorption was found to be about 45° in our experiment. By contrast, the optimal incident angle for the RA absorption is generally in the range of 20°–30°. This is additional evidence to showing that the VH absorption is the main mechanism to account for the extra absorption in our experiments.

IV. HOT ELECTRON MEASUREMENTS

The out-going electron energy spectrum [Fig. 2(A)] generated by the interaction at an intensity of $5\times10^{15}\,\mathrm{W/cm^2}$ was measured directly using the electron magnetic spectrometer placed in the normal direction of the solid target. The spectrum exhibits bi-Maxwellian distribution. The lower hot electron temperature was independent of target materials and was generated by RA mechanism with the scaling law: $T_H(\mathrm{keV}) \approx 6\times10^{-5}(I\lambda^2)^{0.33}$.[14] At the laser intensity of $5\times10^{15}\,\mathrm{W/cm^2}$, it is about 8 keV. This group of electrons is

called bulk plasma electrons by Paul Gibbon in Refs. 11 and 22. Another group of hot electrons with higher temperature about 47 keV at the intensity of $5\times10^{15}\,\mathrm{W/cm^2}$, was generated by the VH process. This bi-Maxwellian hot electron distribution is similar to Paul Gibbon's simulation with mobile-ions.[22] This strongly suggests that the vacuum heating is the main absorption mechanism to heat hot electrons in our experiments. That means at the contrast ratio of 10^5, the VH mechanism is really stimulated and it is the main hot electron heating mechanism.

The hard x-ray spectrum is generally dominated by Bremsstrahlung radiation, which is produced by high energy hot electrons colliding with atom nuclei. The shape and intensity of the Bremsstrahlung radiation is the principle diagnostic for the injecting hot electron flux and temperature[13,23] because the Bremsstrahlung hard x-ray spectrum has the same Maxwellian distribution as colliding electrons. In our experiments, the hard x-ray Bremsstrahlung radiation from injecting electrons was measured by the NaI γ-ray spectrometer. The hard x-ray spectrum also shows a bi-Maxwellian distribution and the hot electron temperature was nearly the same as that measured by the electron spectrometer, shown in Fig. 2(B). The temperature deduced from the hard x-ray spectrum is slightly lower than that from electron spectrum. The reason why the energy of the injecting hot electrons was less than that of out-going electrons might be because the injecting electrons experience deceleration when reentering the solid targets.

V. PIC SIMULATIONS

Simulations using a $1\frac{2}{2}$-dimensional (i.e., x, v_x, v_y, v_z) fully electromagnetic particle in cell (LPIC++) code have been performed, where an electromagnetic wave is launched obliquely from the left-hand side onto an overdense plasma located on the right-hand side with $n_e/n_c=20$, $T_e=200\,\mathrm{eV}$.[21] Based on the simulation results of Paul Gibbon,[22] we chose the ratio of thermal electron temperature to ions as $T_e/T_i=3-5$, and mass ratio $m_i/Zm_e=1836$, original plasma scale length $L=0.004$. A square-sine profile of incident laser pulse was used. Typically 150×2680 electrons and ions and 2680 cells were used. We consider the initial situation in which the ions are mobile and electrons are pulled out into vacuum by the component of the electrical field normal to the target.

Figure 3 shows the electron phase space at $t=12.574$ and $t=13.170$ optical cycles (i.e., electron phase normalized by 2π), respectively. Here we chose $a=0.06$, corresponding an laser intensity of $5\times10^{15}\,\mathrm{W/cm^2}$. We can see another group of electrons accelerated by the laser field appearing at $t=13.170$ after a half of optical cycle, in comparison with the case at $t=12.574$. We also notice most of the electrons heated before cannot return to the target surface in one laser cycle. This implies that these electrons are not quivering in the laser field and a huge electrostatic field (charge separation potential) will be produced by them. It is known that only those electrons ionized in $\omega t=0°-80°$ can return to ions.[24] This suggests that a group of electrons will be pulled out at each optical cycle and an array of electron ''trains''

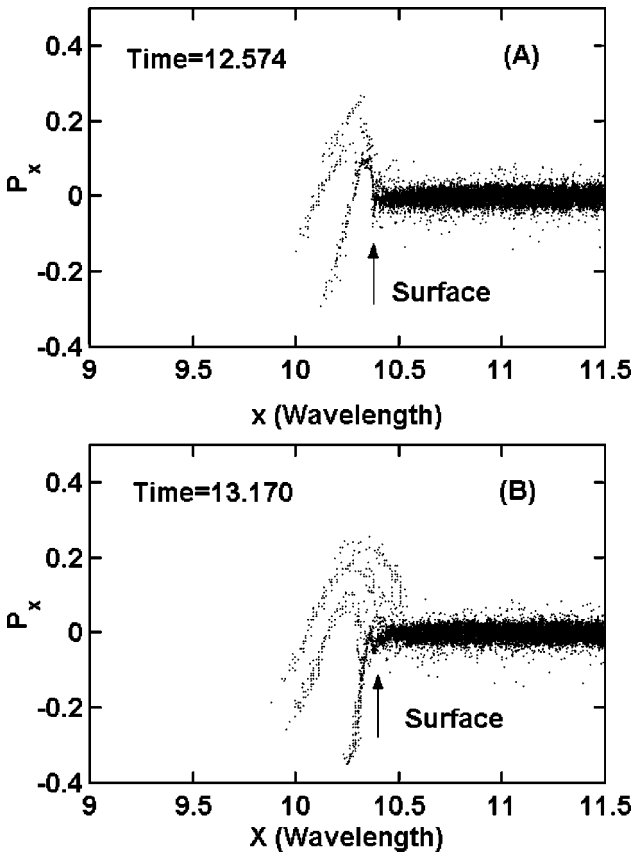

FIG. 3. Simulated electron phase space P_x vs X at $t=12.574$ and 13.170 optical cycle (i.e., electron phase normalized by 2π). $a=0.06$, $L/\lambda=0.004$. The target boundary is at $X=10.3$. P_x is normalized by m_ec. X is normalized by laser wavelength λ.

will be generated in the normal direction of the target surface,[25] forming an electron jet emission in the integrating angular distribution.[26] On the other hand, some of the heated electrons will come back to the target surface, due to the strong charge separation potential, to heat the target plasmas after several optical cycles. This is the accurate picture of the VH.[27]

Figure 4 is the spectrum of electrons heated by laser field

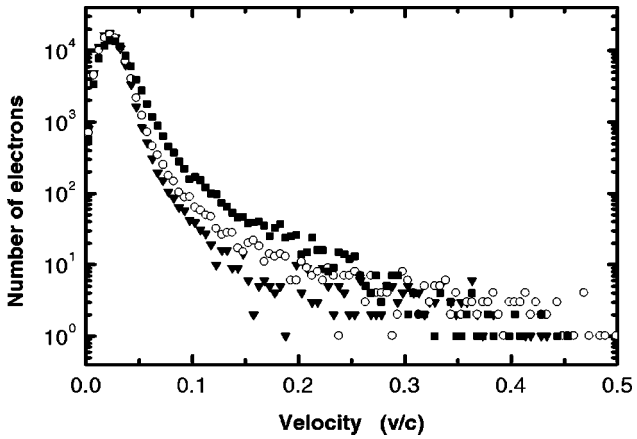

FIG. 4. Simulated spectrum of electrons heated by the laser pulse at $t=15$ (solid downtriangle ▼), 30 (open circle ○), and 70 (solid square ■) optical cycles, respectively.

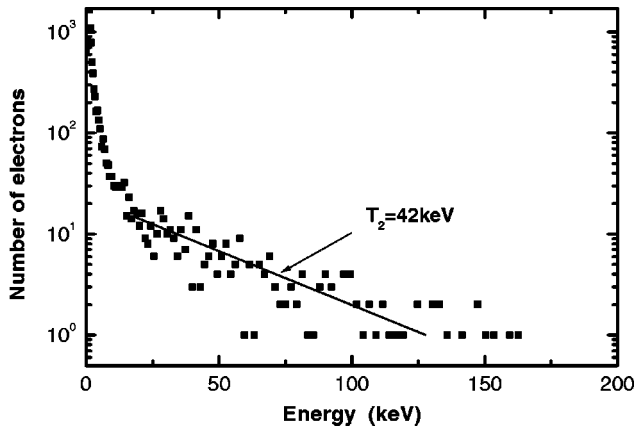

FIG. 5. The time-integrated hot electron spectrum after 75 optical cycles from the PIC simulations.

at different optical cycles. It is apparent that the number of heated electrons increases with interacting time. This demonstrates that the VH is stimulated and heats a group of electrons in each optical cycle. Here we can also see that more electrons with higher energies are generated at the rising edge of the pulse at the curve of $t=30$. This means the laser field accelerates the electrons greatly in the rising edge of laser pulse.

Figure 5 is the time-integrated hot electron energy spectrum after 75 optical cycles, when it is at the end of laser pulse. This is a typical bi-Maxwellian energy distribution. The higher energy hot electron temperature is about 42 keV for $L=0.004\lambda$, $a=0.06$. This agrees well with experimental measurement. In order to check the dependence of temperature on scale-length, the scale-length was changed from 0.001 to 0.07 in the simulations. We found the temperature only slightly changed. The reason is that in this region of scale length, the electrons were accelerated by VH with the total electric field (incident electric field plus reflected electrical field), which is similar for those two scale-lengths, the enhancement of critical surface ($\omega=\omega_p$) field, which is very sensitive to the scale length, is negligible.

VI. CONCLUSIONS

In summary, we have studied the energy absorption, the hot electron generation in the interaction of P-polarized femtosecond laser pulses with Aluminum solid targets. The measurements have suggested that Vacuum Heating is the main heating mechanism for the hot electrons with high energies. The PIC simulations have shown that the hot electrons are pulled out from the target on every optical cycle, forming an electron train-structure in the normal direction of the target. These simulations are consistent with the conclusion that the hot electrons are mainly generated by the vacuum heating process under our experimental conditions.

ACKNOWLEDGMENTS

The authors would like to thank Professor Wei Yu for his valuable discussions.

This work was jointly supported by the National Natural Science Foundation of China (Grant Nos. 19825110, 10005014 and 10075075) and the National Hi-tech ICF Program.

[1] M. D. Perry and G. Mourou, Science **264**, 917 (1994).
[2] R. M. More, Z. Zinamon, K. H. Warren, R. Falcone, and M. Murnane, J. Phys. (Paris), Colloq. **61**, C7-43 (1988).
[3] M. Tabak, J. Hammer, M. E. Glisky, W. L. Kruer, W. C. Wilks, and R. J. Mason, Phys. Plasmas **1**, 1626 (1994).
[4] A. Modena, Z. Najmudin, A. E. Dangor *et al.*, Nature (London) **377**, 606 (1995).
[5] P. A. Norreys, M. Zepf, S. Moustaizis, A. P. Fews, J. Zhang, P. Lee, M. Bakarezos, C. N. Danson, A. Dyson, P. Gibbon, P. Loukakos, D. Neely, F. N. Walsh, J. S. Wark, and A. E. Dangor, Phys. Rev. Lett. **76**, 1832 (1996).
[6] J. D. Kmetec, C. L. Gordon, J. J. Macklin, B. E. Lemoff, G. S. Brown, and S. E. Harris, Phys. Rev. Lett. **68**, 1527 (1992).
[7] T. Ditmire, J. W. G. Tisch, E. Springate, M. B. Mason, N. Hay, R. A. Smith, J. Marangos, and M. H. R. Hutchinson, Nature (London) **386**, 54 (1997); T. D. Donnelly, T. Ditmire, K. Neuman, M. D. Perry, and R. W. Falcone, Phys. Rev. Lett. **76**, 2472 (1996).
[8] H. M. Milchberg, R. R. Freeman, S. C. Davey, and R. M. More, Phys. Rev. Lett. **61**, 2364 (1988); F. Perrot and M. W. C. Dharma-wardana, Phys. Rev. A **36**, 238 (1987); A. Ng, P. Cellier, A. Forsman, R. M. More, T. T. Lee, F. Perrot, M. W. C. Dharma-wardana, and G. A. Rinker, Phys. Rev. Lett. **72**, 3351 (1994).
[9] D. F. Price, R. M. More, R. S. Walling, G. Guethlein, R. L. Shepherd, R. E. Stewart, and W. E. White, Phys. Rev. Lett. **75**, 252 (1995).
[10] F. Brunel, Phys. Rev. Lett. **59**, 52 (1987); Phys. Fluids **31**, 2714 (1998).
[11] P. Gibbon and A. R. Bell, Phys. Rev. Lett. **68**, 1535 (1992); **73**, 664 (1994).
[12] S. Bastiani, A. Rousse, J. P. Geindre, P. Audebert, C. Quoix, G. Hamoniaux, A. Antonetti, and J.-C. Gauthier, Phys. Rev. E **56**, 7179 (1997); S. Bastiani, P. Audebert, J. P. Geindre, Th. Schlegel, C. Guoix, G. Hamoniaux, G. Grillon, and A. Antonetti, *ibid.* **60**, 3439 (1999).
[13] P. Zhang, J. T. He, D. B. Chen, Z. H. Li, Y. Zhang, J. G. Bian, L. Wang, Z. L. Li, B. H. Feng, X. L. Zhang, D. X. Zhang, X. W. Tang, and J. Zhang, Phys. Rev. E **57**, R3746 (1998).
[14] W. L. Kruer, *The Physics of Laser Plasma Interactions* (Addison-Wesley, New York, 1988); S. J. Gitomen, R. D. Jones, F. Begay, A. W. Ehler, J. F. Kephart, and R. Kristal, Phys. Fluids **29**, 2679 (1986); D. W. Forslund, J. M. Kindel, and K. Lee, Phys. Rev. Lett. **39**, 284 (1977).
[15] L. M. Chen, J. Zhang, H. Teng, Q. L. Dong, Z. L. Chen, T. J. Liang, L. Z. Zhao, and Z. Y. Wei, Phys. Rev. E **63**, 036403 (2001).
[16] M. K. Grimes, A. R. Rundquist, Y. S. Lee, and M. C. Downer, Phys. Rev. Lett. **82**, 4010 (1999).
[17] Y. Zhang, J. Zhang, S. H. Pan, and Y. X. Nie, Opt. Commun. **126**, 85 (1996).
[18] E. S. Weibel, Phys. Fluids **10**, 741 (1967); A. A. Andreev, K. Yu. Platonov, and J.-C. Gauthier, Phys. Rev. E **58**, 2424 (1998).
[19] P. J. Catto and R. M. More, Phys. Fluids **20**, 704 (1977); T.-Y. B. Yang, W. L. Kruer, R. M. More, and A. B. Langdon, Phys. Plasmas **2**, 3146 (1995).
[20] T.-Y. B. Yang, W. L. Kruer, A. B. Langdon, and T. W. Johnston, Phys. Plasmas **3**, 2702 (1996).
[21] W. Rozmus, V. T. Tikhonchuk, and R. Cauble, Phys. Plasmas **3**, 360 (1996).
[22] P. Gibbon, Phys. Rev. Lett. **73**, 664 (1994).
[23] M. N. Rousenbluth and R. Z. Sagdeev, *Physics of Laser Plasmas* (North-Holland, Amsterdam, 1991); F. N. Beg, A. R. Bell, A. E. Dangor, C. N. Danson, A. P. Fews, M. E. Glisky, B. A. Hammel, P. Lee, P. A. Norreys, and M. Tatarakis, Phys. Plasmas **4**, 447 (1997).
[24] L. M. Chen, W. Yu, J. Zhang, Z. Y. Chen, and W. M. Jiang, Sci. China A **43**, 1202 (2000).
[25] Y. Sentoku, H. Ruhl, K. Mima, R. Kodama, K. A. Tanaka, and Y. Kishimoto, Phys. Plasmas **6**, 2855 (1999); R. Kodama, K. A. Tanaka, Y. Sentoku, T. Matsushita, H. Fujita, Y. Kitagawa, Y. Kato, T. Yamanaka, and K. Mima, Phys. Rev. Lett. **84**, 674 (2000).
[26] Y. T. Li, J. Zhang, L. M. Chen, J. F. Xia, H. Teng, L. Z. Zhao, J. Q. Lin, Y. J. Li, Z. Y. Wei, L. Wang, and W. M. Jiang, Sci. China A **44**, 98 (2000).
[27] L. H. Cao, W. W. Chang, and Z. W. Yue, Phys. Plasmas **5**, 499 (1998).